

Fast Fractional Programming for Multi-Cell Integrated Sensing and Communications

Yannan Chen, *Student Member, IEEE*, Yi Feng, *Student Member, IEEE*, Xiaoyang Li, *Member, IEEE*, Licheng Zhao, Kaiming Shen, *Senior Member, IEEE*

Abstract—This paper concerns the coordinate multi-cell beamforming design for integrated sensing and communications (ISAC). In particular, we assume that each base station (BS) has massive antennas. The optimization objective is to maximize a weighted sum of the data rates (for communications) and the Fisher information (for sensing). We first show that the conventional beamforming method for the multiple-input multiple-output (MIMO) transmission, i.e., the weighted minimum mean square error (WMMSE) algorithm, has a natural extension to the ISAC problem scenario from a fractional programming (FP) perspective. However, the extended WMMSE algorithm requires computing the $N \times N$ matrix inverse extensively, where N is proportional to the antenna array size, so the algorithm becomes quite costly when antennas are massively deployed. To address this issue, we develop a nonhomogeneous bound and use it in conjunction with the FP technique to solve the ISAC beamforming problem without the need to invert any large matrices. It is further shown that the resulting new FP algorithm has an intimate connection with gradient projection, based on which we can accelerate the convergence via Nesterov’s gradient extrapolation.

Index Terms—Integrated sensing and communication (ISAC), multi-cell beamforming, massive antenna array, large matrix inverse, convergence acceleration.

I. INTRODUCTION

INTEGRATED sensing and communications (ISAC) is an emerging wireless technique that reuses the network infrastructure and radio signals for both communications and sensing—which used to be dealt with separately in the conventional networks, in order to reduce the infrastructure cost and boost the spectral efficiency. This work focuses on the large antenna array case of ISAC, aiming at a system-level optimization by coordinating the antenna beamformers across multiple cells. There are three main results worth noticing about this work. First, we show that the well-known weighted minimum mean square error (WMMSE) algorithm [1], [2], which was initially devised for the multiple-input multiple-output (MIMO) transmission, can be extended for ISAC via the fractional programming (FP) technique, but at a high computation cost due to the large matrix inverse operation. Second, we manage to eliminate all the large matrix inversion from the extended WMMSE by incorporating into FP a generalized

nonhomogeneous bound [3]. Third, the above method turns out to have an intimate connection with gradient projection, so Nesterov’s extrapolation scheme [4] can be used to accelerate its convergence.

The early endeavors in the ISAC field focus on the co-existence of the communication system and the radar system [5]. Nevertheless, the co-existence systems are inefficient in that signal processing is considered separately for communications and sensing. To remedy this defect, the co-existence system evolves into the dual-functional-radar-communication (DFRC) system [6], [7]. Various models have been proposed for the DFRC system in the past few years. One common model is the so-called collocated base station (BS) system, in which the communications function and the sensing function are performed at the same BS [7]. This model is further developed in [8] to account for the broadcast communications toward multiple receivers. For the DFRC model, [8]–[10] consider the point target sensing while [11], [12] consider the extended target sensing. Aside from the collocated BS case, the bi-static BS model has also been extensively studied in the literature to date [13]–[15]. This model assumes that the signal transmission and the echo reception are conducted at two separate BSs; it has further developed into the notion of the multi-static BS system [16], [17]. Regarding the performance metrics, it is popular to use the Fisher information [18], [19], and its reciprocal, i.e., the Cramér-Rao bound (CRB) [13]–[15], to evaluate the performance of sensing. In contrast, the data rate is widely considered for communications [13], [14]. Signal-to-noise ratio (SNR) is another common metric for sensing [8]–[10] and communications [20]–[22]. This work focuses on maximizing a weighted sum of the data rates and the Fisher information in a multi-cell DFRC system with collocated BSs, but it can be readily adapted to other forms of optimization, e.g., maximizing the weighted sum rates under the CRB constraints.

The ISAC beamforming problem (particularly for the DFRC system) is a nontrivial task due to the nonconvex nature of the underlying optimization problem. Quite a few advanced optimization tools have been considered in the previous attempts. Semi-definite relaxation (SDR) is a typical example [8], [10], [22]–[25] because the ISAC beamforming problem can be somehow relaxed in a quadratic form, e.g., as a quadratic semi-definite program (QSDP) [8], a quadratically constrained quadratic program (QSQP) [23], or a semi-definite program (SDP) [10], [22], [24], [25]. Successive convex approximation (SCA) constitutes another popular approach in this area [9], [11], [26], [27]. For example, [11] uses SCA

Manuscript submitted on June 18, 2024.

Yannan Chen, Yi Feng, and Kaiming Shen are with School of Science and Engineering, The Chinese University of Hong Kong (Shenzhen), Shenzhen 518172, China (e-mail: yannanchen@link.cuhk.edu.cn; yifeng@link.cuhk.edu.cn; shenkaiming@cuhk.edu.cn).

Xiaoyang Li and Licheng Zhao are with Shenzhen Research Institute of Big Data, The Chinese University of Hong Kong (Shenzhen), Shenzhen 518172, China. (e-mail: lixiaoyang@sribd.cn; zhaolicheng@sribd.cn).

to convert the ISAC beamforming design to a second-order cone programming (SOCP) problem—which can be efficiently solved by the standard convex optimization method. Another line of studies [28]–[30] utilize the majorization-minimization (MM) theory to make the ISAC beamforming problem convex, especially when the passive beamforming of the intelligent reflecting surface (IRS) is involved. Moreover, because the ISAC beamforming problem is fractionally structured, the fractional programming (FP) technique, i.e., the quadratic transform [31], [32], forms the building block of [15], [33], [34]. Aside from the above model-based optimization approaches, deep learning has become a frontier technique for the ISAC beamforming, e.g., the long short-term memory network [35] and the unconventional convolutional neural network [36].

To exploit the degrees-of-freedom (DoF), the massive MIMO technology has been considered for the ISAC system. In principle, as shown in [37], the efficiency of target detection improves with the antenna array size. From the algorithm design viewpoint, however, the large antenna array can pose a tough challenge. Actually, even considering the communications task alone, the beamforming design with massive antennas is already quite difficult. For instance, although the WMMSE algorithm [1], [2] has been extensively used for the MIMO transmission, it is no longer suited for the massive MIMO case because the algorithm then entails computing the large matrix inverse extensively per iteration. Other standard optimization methods such as SDR and SCA are faced with similar issues since they involve the matrix inverse operation implicitly when performing the interior-point optimization. Some recent efforts aim to improve the efficiency of WMMSE in the massive MIMO case, e.g., [38] proposes a light WMMSE algorithm that has a lower complexity of the matrix inverse computation under certain conditions. The present paper is most closely related to a series of recent works [39], [40] that use a nonhomogeneous bound from [3] to avoid matrix inverse. While [39], [40] focus on the transmit beamforming alone, this work proposes a novel use of the non-homogeneous bound that accounts for both the transmit beamforming and the echo receive beamforming.

The main results of this paper are summarized below:

- In light of the FP technique, we show that the classic algorithm WMMSE [1], [2] for the communications beamforming can be extended for the ISAC beamforming. However, like the original WMMSE, this extended algorithm incurs large matrix inversion when large antenna arrays are deployed.
- After generalizing the non-homogeneous bound in [3] to the linear matrix inequality case, we further use it to eliminate the large matrix inversion from the extended WMMSE algorithm. The resulting algorithm called the non-homogeneous FP method considerably generalizes the results in [39], [40].
- We further show that the non-homogeneous FP method can be interpreted as a gradient projection method [41]. This connection leads us to a novel incorporation of Nesterov’s extrapolation scheme into the FP approach, thereby accelerating the convergence of the ISAC beamforming optimization.

TABLE I
MAIN VARIABLES THROUGHOUT THE PAPER

Symbol	Definition
L	Number of cells/BSs
K	Number of users in each cell
N_ℓ^t	Number of transmit antennas of BS ℓ
N_ℓ^r	Number of radar receive antennas of BS ℓ
$M_{\ell k}$	Number of receive antennas of user (ℓ, k)
$\mathbf{S}_{\ell k}$	Signal intended for user (ℓ, k)
$d_{\ell k}$	Number of data streams for user (ℓ, k)
T	Number of data frames
$\mathbf{W}_{\ell k}$	Beamformer of BS ℓ for its k th user
$\mathbf{H}_{\ell k, i}$	Channel from BS i to user (ℓ, k)
$\Delta_{\ell k}$	Background noise at user (ℓ, k)
σ^2	Background noise power at each user
$\xi_{i\ell}$	Reflection coefficient from BS i to BS ℓ
$\mathbf{a}_\ell^t(\theta_\ell)$	Transmit steering vector of BS ℓ
$\mathbf{a}_\ell^r(\theta_\ell)$	Receive steering vector of BS ℓ
$\tilde{\mathbf{Y}}_\ell$	Echo signal received at BS ℓ
$\tilde{\Delta}$	Background noise at BS ℓ
$\tilde{\sigma}^2$	Background noise power at BS ℓ
$\mathbf{G}_{\ell, i}$	Response matrix

The remainder of this paper is organized as follows. Section II introduces the system model and problem formulation. Section III discusses the joint beamforming design. Section IV presents numerical results. Finally, Section V concludes the paper. Here and throughout, bold lower-case letters represent vectors while bold upper-case letters represent matrices. For a vector \mathbf{a} , \mathbf{a}^H is its conjugate transpose, and $\|\mathbf{a}\|_2$ is its ℓ_2 norm. For a matrix \mathbf{A} , \mathbf{A}^* is its complex conjugate, \mathbf{A}^T is its transpose, \mathbf{A}^H is its conjugate transpose, and $\|\mathbf{A}\|_F$ is its Frobenius norm. For a square matrix \mathbf{A} , $\text{tr}(\mathbf{A})$ is its trace, $|\mathbf{A}|$ is its determinate, and $\lambda_{\max}(\mathbf{A})$ is its largest eigenvalue. For a positive semi-definite matrix \mathbf{A} , $\sqrt{\mathbf{A}}$ is its square root. Denote by \mathbf{I}_d the $d \times d$ identity matrix, \mathbb{C}^ℓ the set of $\ell \times 1$ vectors, $\mathbb{C}^{d \times m}$ the set of $d \times m$ matrices, and $\mathbb{H}_+^{d \times d}$ the set of $d \times d$ positive definite matrices. For a complex number $a \in \mathbb{C}$, $\Re\{a\}$ is its real part, $|a|$ is its absolute value. \otimes stands for the Kronecker product. $\text{vec}(\cdot)$ represents the vectorization operation. The underlined letters represent the collections of the associated vectors or matrices, e.g., for $\mathbf{a}_1, \dots, \mathbf{a}_n \in \mathbb{C}^d$ we write $\underline{\mathbf{a}} = [\mathbf{a}_1, \mathbf{a}_2, \dots, \mathbf{a}_n]^T \in \mathbb{C}^{nd}$. To ease reference, we list the main variables used in this paper in Table I.

II. MULTI-CELL ISAC SYSTEM MODEL

Consider a downlink multi-cell ISAC system with L cells. Assume that each cell has K downlink users. For each BS $\ell = 1, 2, \dots, L$, there are two tasks: (i) send independent messages to the K downlink users in its cell by spatial multiplexing; (ii) detect the direction of arrival (DoA), θ_l , for a point target. An illustrative example of the ISAC system

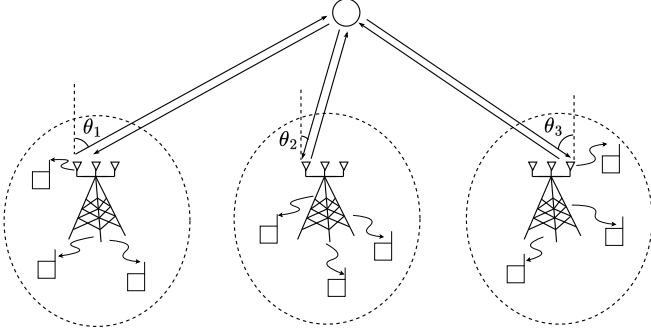


Fig. 1. A multi-cell ISAC system with $L = 3$ and $K = 3$. The circle is the point target to sense. The arrows are the transmit signals and the echo signals.

as described above is shown in Fig. 1. We assume that BS ℓ has N_ℓ^t transmit antennas as well as N_ℓ^r receive antennas for detecting the echos. The k th downlink user in the ℓ th cell is indexed as (ℓ, k) . User (ℓ, k) has $M_{\ell k}$ receive antennas. Notably, the transmit antenna array size N_ℓ^t and the echo antenna array size N_ℓ^r at the BS side can be large, whereas the receive antenna array size $M_{\ell k}$ at the terminal side is often small, as typically assumed for a massive MIMO network.

A. Communications Model

Let $\mathbf{S}_{\ell k} \in \mathbb{C}^{d_{\ell k} \times T}$ be the normalized symbol sequence intended for user (ℓ, k) , where $d_{\ell k}$ is the number of data streams and T is the block length. Note that $d_{\ell k}$ is often small since $d_{\ell k} \leq M_{\ell k}$. Let $\mathbf{W}_{\ell k} \in \mathbb{C}^{N_\ell^t \times d_{\ell k}}$ be the transmit beamformer of BS ℓ for $\mathbf{S}_{\ell k}$. The different data streams are assumed to be statistically independent, i.e.,

$$\frac{1}{T} \mathbb{E}[\mathbf{S}_{\ell k} \mathbf{S}_{\ell k}^H] = \mathbf{I}_{d_{\ell k}}. \quad (1)$$

Denote by $\mathbf{H}_{\ell k, i} \in \mathbb{C}^{M_{\ell k} \times N_i^t}$ the channel from BS i to user (ℓ, k) . Each entry of the background noise $\mathbf{\Delta}_{\ell k} \in \mathbb{C}^{M_{\ell k} \times T}$ is drawn i.i.d. from $\mathcal{CN}(0, \sigma^2)$, and the received signal of user (ℓ, k) is given by

$$\begin{aligned} \mathbf{\Psi}_{\ell k} = & \mathbf{H}_{\ell k, \ell} \mathbf{W}_{\ell k} \mathbf{S}_{\ell k} + \underbrace{\sum_{j \neq k} \mathbf{H}_{\ell k, \ell} \mathbf{W}_{\ell j} \mathbf{S}_{\ell j}}_{\text{intracell interference}} \\ & + \underbrace{\sum_{i \neq \ell} \sum_{j=1}^K \mathbf{H}_{\ell k, i} \mathbf{W}_{ij} \mathbf{S}_{ij}}_{\text{intercell interference}} + \mathbf{\Delta}_{\ell k}. \end{aligned} \quad (2)$$

The data rate for user (ℓ, k) can be computed as

$$R_{\ell k} = \log \left| \mathbf{I}_{d_{\ell k}} + \mathbf{W}_{\ell k}^H \mathbf{H}_{\ell k, \ell}^H \mathbf{F}_{\ell k}^{-1} \mathbf{H}_{\ell k, \ell} \mathbf{W}_{\ell k} \right|, \quad (3)$$

where

$$\begin{aligned} \mathbf{F}_{\ell k} = & \sum_{j \neq k} \mathbf{H}_{\ell k, \ell} \mathbf{W}_{\ell j} \mathbf{W}_{\ell j}^H \mathbf{H}_{\ell k, \ell}^H \\ & + \sum_{i \neq \ell} \sum_{j=1}^K \mathbf{H}_{\ell k, i} \mathbf{W}_{ij} \mathbf{W}_{ij}^H \mathbf{H}_{\ell k, i}^H + \sigma^2 \mathbf{I}_{M_{\ell k}}. \end{aligned} \quad (4)$$

For the good of communications, we wish to maximize the data rates throughout the network.

B. Sensing Model

Recall that BS ℓ has N_ℓ^t transmit antennas (for communications) and N_ℓ^r receive antennas (for sensing). Denote by $\mathbf{a}_\ell^t(\theta_\ell)$ the steering vector of the transmit antennas, $\mathbf{a}_\ell^r(\theta_\ell)$ the steering vector of the receive antennas, and $\xi_{\ell i}$ the reflection coefficient from BS i to BS ℓ . The echo signal $\tilde{\mathbf{\Psi}}_\ell \in \mathbb{C}^{N_\ell^r \times T}$ received at BS ℓ is given by

$$\tilde{\mathbf{\Psi}}_\ell = \sum_{i=1}^L \xi_{\ell i} \mathbf{a}_\ell^r(\theta_\ell) (\mathbf{a}_i^t(\theta_i))^T \left(\sum_{j=1}^K \mathbf{W}_{ij} \mathbf{S}_{ij} \right) + \tilde{\mathbf{\Delta}}_\ell, \quad (5)$$

where each entry of the background noise $\tilde{\mathbf{\Delta}}_\ell \in \mathbb{C}^{N_\ell^r \times T}$ is drawn i.i.d. from $\mathcal{CN}(0, \tilde{\sigma}^2)$. Each BS ℓ recovers the DoA θ_ℓ from the received echo signal $\tilde{\mathbf{Y}}_\ell$.

Mean squared error (MSE) is a common performance metric of estimation. Nevertheless, it is difficult to analyze the MSE of θ_ℓ in our problem case. Instead, we adopt the Fisher information as the performance metric, following the previous works [18], [19] in the ISAC field. Define the response matrix

$$\mathbf{G}_{\ell i} = \xi_{\ell i} \mathbf{a}_\ell^r(\theta_\ell) (\mathbf{a}_i^t(\theta_i))^T, \quad (6)$$

where the transmit steering vector $\mathbf{a}_\ell^t(\theta_\ell)$ and receive steering vector of $\mathbf{a}_\ell^r(\theta_\ell)$ can be specified as

$$\mathbf{a}_\ell^t(\theta_\ell) = [1, e^{-j\pi \sin \theta_\ell}, \dots, e^{-j\pi(N_\ell^t - 1) \sin \theta_\ell}]^T, \quad (7)$$

$$\mathbf{a}_\ell^r(\theta_\ell) = [1, e^{-j\pi \sin \theta_\ell}, \dots, e^{-j\pi(N_\ell^r - 1) \sin \theta_\ell}]^T. \quad (8)$$

Then the vectorization $\tilde{\boldsymbol{\psi}}_\ell = \text{vec}(\tilde{\mathbf{\Psi}}_\ell)$ can be computed as

$$\tilde{\boldsymbol{\psi}}_\ell = \sum_{k=1}^K (\mathbf{I}_T \otimes \mathbf{G}_{\ell k} \mathbf{W}_{\ell k}) \mathbf{s}_{\ell k} + \boldsymbol{\mu}_\ell, \quad (9)$$

where

$$\boldsymbol{\mu}_\ell = \sum_{i=1, i \neq \ell}^L \sum_{j=1}^K (\mathbf{I}_T \otimes \mathbf{G}_{\ell i} \mathbf{W}_{ij}) \mathbf{s}_{ij} + \tilde{\boldsymbol{\delta}}_\ell, \quad (10)$$

$\tilde{\boldsymbol{\delta}}_\ell = \text{vec}(\tilde{\mathbf{\Delta}}_\ell)$, and $\mathbf{s}_{\ell k} = \text{vec}(\mathbf{S}_{\ell k})$. Define \mathbf{Q}_ℓ to be

$$\begin{aligned} \mathbf{Q}_\ell = & \mathbb{E}[\boldsymbol{\mu}_\ell \boldsymbol{\mu}_\ell^H] \\ = & \mathbf{I}_T \otimes \left(\sum_{i=1, i \neq \ell}^L \sum_{j=1}^K \mathbf{G}_{\ell i} \mathbf{W}_{ij} \mathbf{W}_{ij}^H \mathbf{G}_{\ell i}^H + \tilde{\sigma}^2 \mathbf{I}_{N_\ell^r} \right). \end{aligned}$$

Moreover, define $\mathbf{v}_\ell(\theta_\ell) = \sum_{k=1}^K (\mathbf{I}_T \otimes \mathbf{G}_{\ell k} \mathbf{W}_{\ell k}) \mathbf{s}_{\ell k}$. The Fisher information of θ_ℓ is then given by [42]

$$\begin{aligned} J_\ell = & 2 \left(\frac{\partial \mathbf{v}_\ell(\theta_\ell)}{\partial \theta_\ell} \right)^H \mathbf{Q}_\ell^{-1} \frac{\partial \mathbf{v}_\ell(\theta_\ell)}{\partial \theta_\ell} \\ = & 2T \left\{ \sum_{k=1}^K \text{tr} \left((\dot{\mathbf{G}}_{\ell k} \mathbf{W}_{\ell k})^H \hat{\mathbf{Q}}_\ell^{-1} (\dot{\mathbf{G}}_{\ell k} \mathbf{W}_{\ell k}) \right) \right\}, \end{aligned} \quad (11)$$

where $\dot{\mathbf{G}}_{\ell k} = \partial \mathbf{G}_{\ell k} / \partial \theta_\ell$ and

$$\hat{\mathbf{Q}}_\ell = \sum_{i \neq \ell} \sum_{j=1}^K \mathbf{G}_{\ell i} \mathbf{W}_{ij} \mathbf{W}_{ij}^H \mathbf{G}_{\ell i}^H + \tilde{\sigma}^2 \mathbf{I}_{N_\ell^r}. \quad (12)$$

For the good of sensing, we wish to maximize the Fisher information of θ_ℓ at each BS ℓ , which is equivalent to minimizing the Cramér-Rao bound (CRB) on the MSE of θ_ℓ .

C. ISAC Beamforming Problem

To account for both communications and sensing, we consider maximizing a weighted sum of data rates and Fisher information:

$$\underset{\mathbf{W}}{\text{maximize}} \quad \sum_{\ell=1}^L \sum_{k=1}^K \omega_{\ell k} R_{\ell k} + \sum_{\ell=1}^L \beta_\ell J_\ell \quad (13a)$$

$$\text{subject to} \quad \sum_{k=1}^K \|\mathbf{W}_{\ell k}\|_F^2 \leq P_\ell, \quad (13b)$$

where $\omega_{\ell k}, \beta_\ell \geq 0$ are the given nonnegative weights reflecting the priorities of the communications and sensing tasks, and P_ℓ is the power budget of BS ℓ .

III. MAIN RESULTS

As a key observation, problem (13) is fractionally structured, i.e., each $R_{\ell k}$ contains an SINR inside the log-determinant while J_ℓ itself is a ratio, so the FP approach comes into play. In light of this FP interpretation, we first show that the traditional WMMSE algorithm [1], [2] for the communication beamforming can be extended for the ISAC beamforming. However, the complexity of the extended WMMSE algorithm becomes costly in the presence of massive antennas array. To address this issue, we further propose a fast FP algorithm tailored to the ISAC beamforming with massive antennas.

A. Preliminary

We start with a quick review of the (matrix) FP technique, which is the building block of the extended WMMSE algorithm as well as the proposed fast FP algorithm.

For a pair of numerator function $\mathbf{A}_i(x) \in \mathbb{H}_+^{m \times m}$ and denominator function $\mathbf{B}_i(x) \in \mathbb{H}_{++}^{m \times m}$, the matrix ratio between them is

$$\mathbf{M}_i(x) = \sqrt{\mathbf{A}_i^H(x)} \mathbf{B}_i^{-1}(x) \sqrt{\mathbf{A}_i(x)}. \quad (14)$$

where $\sqrt{\mathbf{A}_i(x)} \in \mathbb{C}^{m \times d}$ is the square root of matrix $\mathbf{A}_i(x)$. We now consider n matrix ratios and formulate the *sum-of-weighted-logarithmic-ratios* problem as

$$\underset{x}{\text{maximize}} \quad \sum_{i=1}^n \omega_i \log |\mathbf{I}_m + \mathbf{M}_i(x)| \quad (15a)$$

$$\text{subject to} \quad x \in \mathcal{X}, \quad (15b)$$

with the positive weights $\omega_i > 0$ and a nonempty constraint set \mathcal{X} . It turns out that the matrix ratios can be “moved” to the outside of logarithms.

Proposition 1 (Lagrangian Dual Transform [32]): Problem (15) can be recast to

$$\underset{x, \mathbf{\Gamma}}{\text{maximize}} \quad f_r(x, \mathbf{\Gamma}) \quad (16a)$$

$$\text{subject to} \quad x \in \mathcal{X}, \quad (16b)$$

$$\mathbf{\Gamma}_i \in \mathbb{H}_+^{m \times m}, \quad (16c)$$

where

$$f_r(x, \mathbf{\Gamma}) = \sum_{i=1}^n \omega_i \left(\log |\mathbf{I}_m + \mathbf{\Gamma}_i| - \text{tr}(\mathbf{\Gamma}_i) + \text{tr}(\mathbf{I}_m + \mathbf{\Gamma}_i) \sqrt{\mathbf{A}_i^H(x)} (\mathbf{A}_i(x) + \mathbf{B}_i(x))^{-1} \sqrt{\mathbf{A}_i(x)} \right). \quad (17)$$

Moreover, given a sequence of matrix coefficients $\mathbf{C}_i \in \mathbb{H}_+^{m \times m}$, let us consider the *sum-of-weighted-ratios* problem:

$$\underset{x}{\text{maximize}} \quad \sum_{i=1}^n \omega_i \text{tr}(\mathbf{C}_i \mathbf{M}_i(x)) \quad (18a)$$

$$\text{subject to} \quad x \in \mathcal{X}. \quad (18b)$$

We now decouple the matrix ratios in the above problem.

Proposition 2 (Quadratic Transform [32]): Problem (18) can be recast to

$$\underset{x, \mathbf{Y}}{\text{maximize}} \quad f_q(x, \mathbf{Y}) \quad (19a)$$

$$\text{subject to} \quad x \in \mathcal{X} \quad (19b)$$

$$\mathbf{Y}_i \in \mathbb{C}^{m \times d}, \quad (19c)$$

where

$$f_q(x, \mathbf{Y}) = \sum_{i=1}^n \omega_i \text{tr} \left(2\Re \left\{ \sqrt{\mathbf{A}_i^H(x)} \mathbf{Y}_i \mathbf{C}_i \right\} - \mathbf{Y}_i^H \mathbf{B}_i(x) \mathbf{Y}_i \mathbf{C}_i \right). \quad (20)$$

We remark that the above proposition slightly extends the original form of the quadratic transform in [32] by incorporating the matrix coefficients \mathbf{C}_i .

B. Extended WMMSE for ISAC Beamforming

We now return to the ISAC beamforming problem in (13). Our goal here is to extend the WMMSE algorithm for the ISAC beamforming by using the FP technique from Proposition 1 and Proposition 2. First, we use the Lagrangian dual transform in Proposition 1 to move the ratios to the outside of log-determinants for the term $\sum_{\ell=1}^L \sum_{k=1}^K \omega_{\ell k} R_{\ell k}$ in (13a). As a result, problem (13) is converted to

$$\underset{\mathbf{W}, \mathbf{\Gamma}}{\text{maximize}} \quad f_r(\mathbf{W}, \mathbf{\Gamma}) + \sum_{\ell=1}^L \beta_\ell J_\ell \quad (21a)$$

$$\text{subject to} \quad \sum_{k=1}^K \|\mathbf{W}_{\ell k}\|_F^2 \leq P_\ell \quad (21b)$$

$$\mathbf{\Gamma}_{\ell k} \in \mathbb{H}_+^{d_{\ell k} \times d_{\ell k}}, \quad (21c)$$

where

$$f_r(\mathbf{W}, \mathbf{\Gamma}) = \sum_{\ell=1}^L \sum_{k=1}^K \omega_{\ell k} \left[\log |\mathbf{I}_{d_{\ell k}} + \mathbf{\Gamma}_{\ell k}| - \text{tr}(\mathbf{\Gamma}_{\ell k}) + \text{tr} \left((\mathbf{I}_{d_{\ell k}} + \mathbf{\Gamma}_{\ell k}) \mathbf{W}_{\ell k}^H \mathbf{H}_{\ell k, \ell}^H \mathbf{U}_{\ell k}^{-1} \mathbf{H}_{\ell k, \ell} \mathbf{W}_{\ell k} \right) \right] \quad (22)$$

and

$$\mathbf{U}_{\ell k} = \sum_{i=1}^L \sum_{j=1}^K \mathbf{H}_{\ell k, i} \mathbf{W}_{ij} \mathbf{W}_{ij}^H \mathbf{H}_{\ell k, i}^H + \sigma^2 \mathbf{I}_{M_{\ell k}}. \quad (23)$$

$$f_q(\underline{\mathbf{W}}, \underline{\mathbf{\Gamma}}, \underline{\mathbf{Y}}, \underline{\tilde{\mathbf{Y}}}) = \sum_{\ell, k} \left[\text{tr}(2\Re\{\mathbf{W}_{\ell k}^H \mathbf{\Lambda}_{\ell k}\}) - \omega_{\ell k} \mathbf{Y}_{\ell k}^H \mathbf{U}_{\ell k} \mathbf{Y}_{\ell k} (\mathbf{I} + \mathbf{\Gamma}_{\ell k}) - 2T\beta_{\ell} \tilde{\mathbf{Y}}_{\ell k}^H \hat{\mathbf{Q}}_{\ell} \tilde{\mathbf{Y}}_{\ell k} \right] + \omega_{\ell k} \log |\mathbf{I} + \mathbf{\Gamma}_{\ell k}| - \text{tr}(\omega_{\ell k} \mathbf{\Gamma}_{\ell k}) \quad (25)$$

When $\underline{\mathbf{W}}$ is fixed, the new problem (21) is convex in $\underline{\mathbf{\Gamma}}$. According to the first-order condition, each $\mathbf{\Gamma}_{\ell k}$ can be optimally determined as

$$\mathbf{\Gamma}_{\ell k}^* = \mathbf{W}_{\ell k}^H \mathbf{H}_{\ell k, \ell}^H \mathbf{F}_{\ell k}^{-1} \mathbf{H}_{\ell k, \ell} \mathbf{W}_{\ell k}. \quad (24)$$

We now consider optimizing $\underline{\mathbf{W}}$ for fixed $\underline{\mathbf{\Gamma}}$.

Notice that (21) is a sum-of-weighted-ratios problem of $\underline{\mathbf{W}}$ when $\underline{\mathbf{\Gamma}}$ is fixed, so the quadratic transform from Proposition 2 is applicable. The optimization objective in (21a) is then further recast to $f_q(\underline{\mathbf{W}}, \underline{\mathbf{\Gamma}}, \underline{\mathbf{Y}}, \underline{\tilde{\mathbf{Y}}})$ as shown in (25) with

$$\mathbf{\Lambda}_{\ell k} = \omega_{\ell k} \mathbf{H}_{\ell k, \ell}^H \mathbf{Y}_{\ell k} (\mathbf{I}_{d_{\ell k}} + \mathbf{\Gamma}_{\ell k}) + 2T\beta_{\ell} \hat{\mathbf{G}}_{\ell}^H \tilde{\mathbf{Y}}_{\ell k}. \quad (26)$$

For the notational clarity in (25), we use $\mathbf{Y}_{\ell k}$ to denote each auxiliary variable introduced (by the quadratic transform) for the matrix ratios related to the communication task, and use $\tilde{\mathbf{Y}}_{\ell k}$ to denote each auxiliary variable introduced for the matrix ratios related to the sensing task. The resulting further reformulation of problem (21) is

$$\underset{\underline{\mathbf{W}}, \underline{\mathbf{\Gamma}}, \underline{\mathbf{Y}}, \underline{\tilde{\mathbf{Y}}}}{\text{maximize}} \quad f_q(\underline{\mathbf{W}}, \underline{\mathbf{\Gamma}}, \underline{\mathbf{Y}}, \underline{\tilde{\mathbf{Y}}}) \quad (27a)$$

$$\text{subject to} \quad \sum_{k=1}^K \|\mathbf{W}_{\ell k}\|_F^2 \leq P_{\ell}, \quad \forall \ell \quad (27b)$$

$$\mathbf{\Gamma}_{\ell k} \in \mathbb{H}_+^{d_{\ell k} \times d_{\ell k}} \quad (27c)$$

$$\mathbf{Y}_{\ell k} \in \mathbb{C}^{M_{\ell k} \times d_{\ell k}} \quad (27d)$$

$$\tilde{\mathbf{Y}}_{\ell k} \in \mathbb{C}^{N_{\ell}^r \times d_{\ell k}}. \quad (27e)$$

When $\underline{\mathbf{W}}$ and $\underline{\mathbf{\Gamma}}$ are both held fixed, the above problem is jointly convex in $\underline{\mathbf{Y}}$ and $\underline{\tilde{\mathbf{Y}}}$, so we can optimally determine them by the first-order condition as

$$\mathbf{Y}_{\ell k}^* = \mathbf{U}_{\ell k}^{-1} \mathbf{H}_{\ell k, \ell} \mathbf{W}_{\ell k}, \quad (28)$$

$$\tilde{\mathbf{Y}}_{\ell k}^* = \hat{\mathbf{Q}}_{\ell}^{-1} \hat{\mathbf{G}}_{\ell} \mathbf{W}_{\ell k}. \quad (29)$$

We then aim to optimize $\underline{\mathbf{W}}$ with the rest variables held fixed. Toward this end, we rewrite $f_q(\underline{\mathbf{W}}, \underline{\mathbf{\Gamma}}, \underline{\mathbf{Y}}, \underline{\tilde{\mathbf{Y}}})$ as

$$f_q(\underline{\mathbf{W}}, \underline{\mathbf{\Gamma}}, \underline{\mathbf{Y}}, \underline{\tilde{\mathbf{Y}}}) = \sum_{\ell, k} \text{tr}(2\Re\{\mathbf{W}_{\ell k}^H \mathbf{\Lambda}_{\ell k}\}) - \mathbf{W}_{\ell k}^H \mathbf{L}_{\ell} \mathbf{W}_{\ell k} + \text{const}, \quad (30)$$

where const is a constant term when $(\underline{\mathbf{\Gamma}}, \underline{\mathbf{Y}}, \underline{\tilde{\mathbf{Y}}})$ are fixed, and

$$\mathbf{L}_{\ell} = \sum_{i=1}^L \sum_{j=1}^K \omega_{ij} \mathbf{H}_{ij}^H \mathbf{Y}_{ij} (\mathbf{I}_{d_{ij}} + \mathbf{\Gamma}_{ij}) \mathbf{Y}_{ij}^H \mathbf{H}_{ij, \ell} + 2T \sum_{i=1, i \neq \ell}^L \sum_{j=1}^K \mathbf{G}_{i\ell}^H (\beta_i \tilde{\mathbf{Y}}_{ij} \tilde{\mathbf{Y}}_{ij}^H) \mathbf{G}_{i\ell}. \quad (31)$$

By the identity $\text{tr}(\mathbf{A}\mathbf{A}^H) = \|\mathbf{A}\|_F^2$, we get the optimal $\mathbf{W}_{\ell k}$:

$$\mathbf{W}_{\ell k}^* = \arg \min_{\underline{\mathbf{W}} \in \mathcal{W}} \|\mathbf{L}_{\ell}^{\frac{1}{2}} (\mathbf{W}_{\ell k} - \mathbf{L}_{\ell}^{-1} \mathbf{\Lambda}_{\ell k})\|_F^2. \quad (32)$$

Algorithm 1 Extended WMMSE for ISAC Beamforming

- 1: Initialize $\underline{\mathbf{W}}$ to a feasible value.
 - 2: **repeat**
 - 3: Update each $\mathbf{\Gamma}_{\ell k}$ by (24).
 - 4: Update each $\mathbf{Y}_{\ell k}$ and $\tilde{\mathbf{Y}}_{\ell k}$ by (28) and (29), respectively.
 - 5: Update each $\mathbf{W}_{\ell k}$ by (34).
 - 6: **until** the objective value converges
-

where

$$\mathcal{W} = \left\{ \underline{\mathbf{W}} : \sum_{k=1}^K \|\mathbf{W}_{\ell k}\|_F^2 \leq P_{\ell}, \quad \forall \ell \right\} \quad (33)$$

is the feasible set. The above solution can be further written as

$$\mathbf{W}_{\ell k}^* = \left(\eta_{\ell} \mathbf{I}_{N_{\ell}^t} + \mathbf{L}_{\ell} \right)^{-1} \mathbf{\Lambda}_{\ell k}, \quad (34)$$

where the Lagrange multiplier η_{ℓ} accounts for the power constraint and can be optimally determined as

$$\eta_{\ell} = \min \left\{ \eta \geq 0 : \sum_{k=1}^K \|\mathbf{W}_{\ell k}(\eta)\|_F^2 \leq P_{\ell} \right\}. \quad (35)$$

We summarize the above iterative optimization steps in Algorithm 1. In the following two remarks, we show that Algorithm 1 is a generalization of the well-known WMMSE algorithm [2], and also point out the bottleneck of Algorithm 1.

Remark 1: If each $\beta_{\ell} = 0$, i.e., when we consider maximizing the weighted sum rates alone, then Algorithm 1 reduces to the WMMSE algorithm [1], [2]. Nevertheless, the WMMSE was initially proposed in [1] based on a duality between the rate maximization and the MSE minimization, whereas we rederive it by using the FP technique.

Remark 2: Notice that updating $\underline{\mathbf{W}}$ as in (34) and updating $\underline{\tilde{\mathbf{Y}}}$ as in (29) all entail computing the matrix inverses, which can be quite costly when massive antennas are deployed so that N_{ℓ}^r or/and N_{ℓ}^t is large. The fast FP algorithm as proposed in Section III-C is motivated in part to eliminate the matrix inverse operation.

C. Large Matrix Inverse Elimination

Before tackling the large matrix inverse issue of the ISAC beamforming problem, we first illustrate how this issue can be addressed in a toy example. The main tool is stated in the following lemma:

Lemma 1 (Nonhomogeneous Bound): Suppose that the two Hermitian matrices $\mathbf{L}, \mathbf{K} \in \mathbb{C}^{d \times d}$ satisfy $\mathbf{L} \preceq \mathbf{K}$, e.g., when $\mathbf{K} = \lambda \mathbf{I}$ where $\lambda = \lambda_{\max}(\mathbf{L})$. Then for any two matrices $\mathbf{X}, \mathbf{Z} \in \mathbb{C}^{d \times m}$, one has

$$\text{tr}(\mathbf{X}^H \mathbf{L} \mathbf{X}) \leq \text{tr}(\mathbf{X}^H \mathbf{K} \mathbf{X} + 2\Re\{\mathbf{X}^H (\mathbf{L} - \mathbf{K}) \mathbf{Z}\} + \mathbf{Z}^H (\mathbf{K} - \mathbf{L}) \mathbf{Z}), \quad (36)$$

where the equality holds if $\mathbf{Z} = \mathbf{X}$.

Proof: Because $f(\mathbf{X}) = \text{tr}(\mathbf{X}^H(\mathbf{K} - \mathbf{L})\mathbf{X})$ is convex, we have

$$f(\mathbf{X}) \geq f(\mathbf{Z}) + \Re\{\text{tr}[(\nabla f(\mathbf{Z}))^\top(\mathbf{X} - \mathbf{Z})]\},$$

where $\nabla f(\mathbf{Z}) = 2(\mathbf{K} - \mathbf{L})^\top \mathbf{Z}^*$. The above inequality gives (36). \blacksquare

We remark that the above lemma generalizes the result of Example 13 in [3]. The remainder of Section III-C shows how Lemma 1 can be used to eliminate the matrix inverse from the iterative optimization of a single-ratio problem. Then Section III-D extends this result to the multi-ratio case in the ISAC beamforming problem.

Example 1: Consider the following single-ratio problem:

$$\underset{\mathbf{X}}{\text{maximize}} \quad \text{tr}((\mathbf{A}\mathbf{X})^H(\mathbf{B}\mathbf{X}\mathbf{X}^H\mathbf{B}^H)^{-1}(\mathbf{A}\mathbf{X})) \quad (37a)$$

$$\text{subject to} \quad \mathbf{X} \in \mathcal{X}. \quad (37b)$$

where $\mathbf{A} \in \mathbb{C}^{n \times d}$, $\mathbf{B} \in \mathbb{C}^{n \times d}$, $\mathbf{X} \in \mathbb{C}^{d \times m}$, and \mathcal{X} is a nonempty constraint set on \mathbf{X} . By the quadratic transform in Proposition 2, the above problem can be recast to

$$\underset{\mathbf{X}, \mathbf{Y}}{\text{maximize}} \quad f_q(\mathbf{X}, \mathbf{Y}) \quad (38a)$$

$$\text{subject to} \quad \mathbf{X} \in \mathcal{X} \quad (38b)$$

$$\mathbf{Y} \in \mathbb{C}^{n \times m}, \quad (38c)$$

where the new objective function is

$$f_q(\mathbf{X}, \mathbf{Y}) = \text{tr}(2\Re\{\mathbf{X}^H(\mathbf{A}^H\mathbf{Y})\} - \mathbf{X}^H(\mathbf{B}^H\mathbf{Y}\mathbf{Y}^H\mathbf{B})\mathbf{X}). \quad (39)$$

If we optimize \mathbf{X} and \mathbf{Y} iteratively in the above new problem, then both \mathbf{X} and \mathbf{Y} can be optimally updated in closed form by completing the square in $f_q(\mathbf{X}, \mathbf{Y})$. However, these optimal updates incur the matrix inverse operation, which can be computationally costly when n and d are large. The conventional WMMSE algorithm is faced with the same issue.

Now we propose reformulating problem (38) further by the nonhomogeneous bound in Lemma 1. Treating

$$\mathbf{L} = \mathbf{B}^H\mathbf{Y}\mathbf{Y}^H\mathbf{B}, \quad (40)$$

we can convert problem (38) to

$$\underset{\mathbf{X}, \mathbf{Y}, \mathbf{Z}}{\text{maximize}} \quad g_o(\mathbf{X}, \mathbf{Y}, \mathbf{Z}) \quad (41a)$$

$$\text{subject to} \quad \mathbf{X} \in \mathcal{X} \quad (41b)$$

$$\mathbf{Y} \in \mathbb{C}^{n \times m} \quad (41c)$$

$$\mathbf{Z} \in \mathbb{C}^{d \times m}, \quad (41d)$$

where the new objective function is

$$g_o(\mathbf{X}, \mathbf{Y}, \mathbf{Z}) = \text{tr}\left(2\Re\{\mathbf{X}^H(\mathbf{A}^H\mathbf{Y})\} + \mathbf{X}^H(\lambda\mathbf{I}_d - \mathbf{L})\mathbf{Z}\right. \\ \left. + \mathbf{Z}^H(\mathbf{L} - \lambda\mathbf{I}_d)\mathbf{Z} - \lambda\mathbf{X}^H\mathbf{X}\right), \quad (42)$$

where $\lambda = \lambda_{\max}(\mathbf{L})$. Notice that \mathbf{X} can now be optimally determined for $g_o(\mathbf{X}, \mathbf{Y}, \mathbf{Z})$ in closed form without computing the matrix inverse when the other variables (\mathbf{Y}, \mathbf{Z}) are held fixed. This desirable result motivates us to apply Lemma 1 one more time in order to get rid of the matrix inverse for the

optimal update of \mathbf{Y} in solving (41). Specifically, rewriting (42) as

$$g_o(\mathbf{X}, \mathbf{Y}, \mathbf{Z}) = \text{tr}\left(\Re\{-\mathbf{Y}^H(\mathbf{B}\mathbf{Z}(2\mathbf{X} - \mathbf{Z})^H\mathbf{B}^H)\mathbf{Y}\right. \\ \left.+ 2\mathbf{Y}^H(\mathbf{A}\mathbf{X}) + \lambda(2\mathbf{X}^H\mathbf{Z} - \mathbf{X}^H\mathbf{X} - \mathbf{Z}^H\mathbf{Z})\right) \quad (43)$$

and treating

$$\tilde{\mathbf{L}} = \mathbf{B}\mathbf{Z}(2\mathbf{X} - \mathbf{Z})^H\mathbf{B}^H, \quad (44)$$

we further recast problem (41) to

$$\underset{\mathbf{X}, \mathbf{Y}, \mathbf{Z}, \tilde{\mathbf{Z}}}{\text{maximize}} \quad g_s(\mathbf{X}, \mathbf{Y}, \mathbf{Z}, \tilde{\mathbf{Z}}) \quad (45a)$$

$$\text{subject to} \quad \mathbf{X} \in \mathcal{X} \quad (45b)$$

$$\mathbf{Y} \in \mathbb{C}^{n \times m} \quad (45c)$$

$$\mathbf{Z} \in \mathbb{C}^{d \times m} \quad (45d)$$

$$\tilde{\mathbf{Z}} \in \mathbb{C}^{n \times m}, \quad (45e)$$

where

$$g_s(\mathbf{X}, \mathbf{Y}, \mathbf{Z}, \tilde{\mathbf{Z}}) = \text{tr}\left(\Re\{2\mathbf{Y}^H(\mathbf{A}\mathbf{X} + (\tilde{\lambda}\mathbf{I}_n - \tilde{\mathbf{L}})\tilde{\mathbf{Z}})\right. \\ \left.+ \tilde{\mathbf{Z}}^H(\tilde{\mathbf{L}} - \tilde{\lambda}\mathbf{I}_n)\tilde{\mathbf{Z}} + \lambda(2\mathbf{X}^H\mathbf{Z} - \mathbf{X}^H\mathbf{X} - \mathbf{Z}^H\mathbf{Z})\right. \\ \left.- \tilde{\lambda}\mathbf{Y}\mathbf{Y}^H\right) \quad (46)$$

with $\tilde{\lambda} = \lambda_{\max}(\tilde{\mathbf{L}})$. We propose optimizing the variables of $g_s(\mathbf{X}, \mathbf{Y}, \mathbf{Z}, \tilde{\mathbf{Z}})$ in an iterative fashion as

$$\dots \rightarrow \mathbf{X}^\tau \rightarrow \mathbf{Z}^\tau \rightarrow \mathbf{Y}^\tau \rightarrow \tilde{\mathbf{Z}}^\tau \rightarrow \mathbf{X}^{\tau+1} \rightarrow \dots$$

We now specify the iterative optimization steps. First, according to Lemma 1, \mathbf{Z} and $\tilde{\mathbf{Z}}$ are optimally updated as

$$\mathbf{Z}^* = \mathbf{X}, \quad (47)$$

$$\tilde{\mathbf{Z}}^* = \mathbf{Y}. \quad (48)$$

With the optimal $\tilde{\mathbf{Z}}^* = \mathbf{Y}$ plugged in $g_s(\mathbf{X}, \mathbf{Y}, \tilde{\mathbf{Z}}, \mathbf{Z})$, we can find the optimal update of \mathbf{X} by completing the square as

$$\mathbf{X}^* = \|\lambda\mathbf{X} - \mathbf{A}^H\mathbf{Y} - (\lambda\mathbf{I}_d - \mathbf{L})\mathbf{Z}\|_F^2 \\ = \mathbf{Z} + \frac{1}{\lambda}(\mathbf{A}^H\mathbf{Y} - \mathbf{L}\mathbf{Z}). \quad (49)$$

Likewise, after \mathbf{Z} has been optimally updated to \mathbf{X} , we can find the optimal update of \mathbf{Y} by completing the square as

$$\mathbf{Y}^* = \arg \min \|\tilde{\lambda}\mathbf{Y} - \mathbf{A}\mathbf{X} - (\tilde{\lambda}\mathbf{I}_n - \tilde{\mathbf{L}})\tilde{\mathbf{Z}}\|_F^2 \\ = \tilde{\mathbf{Z}} + \frac{1}{\tilde{\lambda}}(\mathbf{A}\mathbf{X} - \tilde{\mathbf{L}}\tilde{\mathbf{Z}}). \quad (50)$$

We remark that the above iterative optimization steps do not incur any matrix inverse.

D. Nonhomogeneous FP for ISAC Beamforming

We now extend the result of Example 1 to the multi-ratio FP case for the ISAC beamforming. First, we still apply the Lagrangian dual transform in Proposition 1 to problem (13) as formerly shown in Section III-B, so that the original problem is converted to (21). With $\underline{\mathbf{L}}$ iteratively updated as in (24), solving for $\underline{\mathbf{W}}$ in (21) boils down to a sum-of-ratios problem.

Again, we then decouple each ratio by the quadratic transform in Proposition 2. The resulting further reformulated

$$g_o(\underline{\mathbf{W}}, \underline{\mathbf{\Gamma}}, \underline{\mathbf{Y}}, \underline{\tilde{\mathbf{Y}}}, \underline{\mathbf{Z}}) = \sum_{\ell, k} \left[\text{tr} \left(2\Re \{ \mathbf{W}_{\ell k}^H \mathbf{\Lambda}_{\ell k} + \mathbf{W}_{\ell k}^H (\lambda_\ell \mathbf{I}_{N_\ell^t} - \mathbf{L}_\ell) \mathbf{Z}_{\ell k} \} + \mathbf{Z}_{\ell k}^H (\mathbf{L}_\ell - \lambda_\ell \mathbf{I}_{N_\ell^t}) \mathbf{Z}_{\ell k} - \lambda_\ell \mathbf{W}_{\ell k}^H \mathbf{W}_{\ell k} \right) \right. \\ \left. - \text{tr} \left(2\tilde{\sigma}^2 T \beta_\ell \tilde{\mathbf{Y}}_{\ell k}^H \tilde{\mathbf{Y}}_{\ell k} + \omega_{\ell k} \sigma^2 (\mathbf{I}_{d_{\ell k}} + \mathbf{\Gamma}_{\ell k}) \mathbf{Y}_{\ell k}^H \mathbf{Y}_{\ell k} \right) + \omega_{\ell k} \log |\mathbf{I}_{d_{\ell k}} + \mathbf{\Gamma}_{\ell k}| - \text{tr}(\omega_{\ell k} \mathbf{\Gamma}_{\ell k}) \right] \quad (52)$$

$$g_s(\underline{\mathbf{W}}, \underline{\mathbf{\Gamma}}, \underline{\mathbf{Y}}, \underline{\tilde{\mathbf{Y}}}, \underline{\mathbf{Z}}, \underline{\tilde{\mathbf{Z}}}) = \sum_{\ell, k} \left[\text{tr} \left(\Re \{ 2\mathbf{W}_{\ell k}^H \mathbf{\Lambda}_{\ell k} + 2\tilde{\mathbf{Y}}_{\ell k}^H (\tilde{\lambda}_\ell \mathbf{I}_{N_\ell^r} - \tilde{\mathbf{L}}_\ell) \tilde{\mathbf{Z}}_{\ell k} + \tilde{\mathbf{Z}}_{\ell k}^H (\tilde{\mathbf{L}}_\ell - \tilde{\lambda}_\ell \mathbf{I}_{N_\ell^r}) \tilde{\mathbf{Z}}_{\ell k} - (2\mathbf{W}_{\ell k} - \mathbf{Z}_{\ell k})^H \mathbf{D}_\ell \mathbf{Z}_{\ell k} \right. \right. \\ \left. \left. + \lambda_\ell (2\mathbf{W}_{\ell k}^H \mathbf{Z}_{\ell k} - \mathbf{Z}_{\ell k}^H \mathbf{Z}_{\ell k} - \mathbf{W}_{\ell k}^H \mathbf{W}_{\ell k}) \right) \right] + \omega_{\ell k} \log |\mathbf{I}_{d_{\ell k}} + \mathbf{\Gamma}_{\ell k}| - \text{tr}(\omega_{\ell k} \mathbf{\Gamma}_{\ell k} + \omega_{\ell k} \sigma^2 (\mathbf{I}_{d_{\ell k}} + \mathbf{\Gamma}_{\ell k}) \mathbf{Y}_{\ell k}^H \mathbf{Y}_{\ell k}) \quad (56)$$

problem is formerly shown in (27). Recall that if we stop here and consider optimizing the primal variable $\underline{\mathbf{W}}$ along with the auxiliary variables $(\underline{\mathbf{\Gamma}}, \underline{\mathbf{Y}}, \underline{\tilde{\mathbf{Y}}})$ in an iterative fashion, then we end up with an extended WMMSE algorithm—which incurs large matrix inverse.

In order to get rid of large matrix inverse, we follow the procedure in Example 1 and reformulate problem (27) further. Treating each \mathbf{L}_ℓ in (31) as \mathbf{L} in (36), we can use Lemma 1 to reformulate problem (27) as

$$\underset{\underline{\mathbf{W}}, \underline{\mathbf{\Gamma}}, \underline{\mathbf{Y}}, \underline{\tilde{\mathbf{Y}}}, \underline{\mathbf{Z}}}{\text{maximize}} \quad g_o(\underline{\mathbf{W}}, \underline{\mathbf{\Gamma}}, \underline{\mathbf{Y}}, \underline{\tilde{\mathbf{Y}}}, \underline{\mathbf{Z}}) \quad (51a)$$

$$\text{subject to} \quad \underline{\mathbf{W}} \in \mathcal{W} \quad (51b)$$

$$\mathbf{\Gamma}_{\ell k} \in \mathbb{H}_+^{d_{\ell k} \times d_{\ell k}} \quad (51c)$$

$$\mathbf{Y}_{\ell k} \in \mathbb{C}^{M_{\ell k} \times d_{\ell k}} \quad (51d)$$

$$\tilde{\mathbf{Y}}_{\ell k} \in \mathbb{C}^{N_\ell^r \times d_{\ell k}} \quad (51e)$$

$$\mathbf{Z}_{\ell k} \in \mathbb{C}^{N_\ell^t \times d_{\ell k}}, \quad (51f)$$

where the new objective function $g_o(\underline{\mathbf{W}}, \underline{\mathbf{\Gamma}}, \underline{\mathbf{Y}}, \underline{\tilde{\mathbf{Y}}}, \underline{\mathbf{Z}})$ is shown in (52) as displayed at the top of the page with $\lambda_\ell = \lambda_{\max}(\mathbf{L}_\ell)$. Note that the above $g_o(\underline{\mathbf{W}}, \underline{\mathbf{\Gamma}}, \underline{\mathbf{Y}}, \underline{\tilde{\mathbf{Y}}}, \underline{\mathbf{Z}})$ can be thought of as a multi-ratio generalization of the previous $g_o(\mathbf{X}, \mathbf{Y}, \mathbf{Z})$ in (42) in Example 1.

Next, defining

$$\mathbf{D}_\ell = \sum_{i=1}^L \sum_{j=1}^K \omega_{\ell j} \mathbf{H}_{ij, \ell}^H \mathbf{Y}_{ij} (\mathbf{I}_{d_{ij}} + \mathbf{\Gamma}_{ij}) \mathbf{Y}_{ij}^H \mathbf{H}_{ij, \ell}, \quad (53)$$

and treating

$$\tilde{\mathbf{L}}_\ell = 2T \sum_{i=1, i \neq \ell}^L \sum_{j=1}^K \mathbf{G}_{i\ell} (\beta_i \mathbf{Z}_{ij} (2\mathbf{W}_{ij} - \mathbf{Z}_{ij})^H) \mathbf{G}_{i\ell}^H \\ + \tilde{\sigma}^2 \mathbf{I}_{N_\ell^r} \quad (54)$$

for each ℓ as \mathbf{L} in (36), we use Lemma 1 to further reformulate (51) as

$$\underset{\underline{\mathbf{W}}, \underline{\mathbf{\Gamma}}, \underline{\mathbf{Y}}, \underline{\tilde{\mathbf{Y}}}, \underline{\mathbf{Z}}, \underline{\tilde{\mathbf{Z}}}}{\text{maximize}} \quad g_s(\underline{\mathbf{W}}, \underline{\mathbf{\Gamma}}, \underline{\mathbf{Y}}, \underline{\tilde{\mathbf{Y}}}, \underline{\mathbf{Z}}, \underline{\tilde{\mathbf{Z}}}) \quad (55a)$$

$$\text{subject to} \quad (51b) - (51f) \quad (55b)$$

$$\tilde{\mathbf{Z}}_{\ell k} \in \mathbb{C}^{N_\ell^r \times d_{\ell k}}, \quad (55c)$$

where the new objective function is shown in (56) as displayed at the top of the page with $\tilde{\lambda}_\ell = \lambda_{\max}(\tilde{\mathbf{L}}_\ell)$. The above is the ultimate problem reformulation.

Now, following the steps in Example 1, we consider optimizing the variables in (55) iteratively as

$$\cdots \rightarrow \underline{\mathbf{W}} \rightarrow \underline{\mathbf{Z}} \rightarrow \underline{\mathbf{\Gamma}} \rightarrow \underline{\mathbf{Y}} \rightarrow \underline{\tilde{\mathbf{Y}}} \rightarrow \underline{\tilde{\mathbf{Z}}} \rightarrow \underline{\mathbf{W}} \rightarrow \cdots$$

According to Lemma 1, $\underline{\mathbf{Z}}$ and $\underline{\tilde{\mathbf{Z}}}$ are optimally updated as

$$\mathbf{Z}_{\ell k}^* = \mathbf{W}_{\ell k}, \quad (57)$$

$$\tilde{\mathbf{Z}}_{\ell k}^* = \tilde{\mathbf{Y}}_{\ell k}. \quad (58)$$

When other variables are held fixed, $\underline{\mathbf{\Gamma}}$ is still optimally determined as in (24) by solving $\partial g_s / \partial \underline{\mathbf{\Gamma}}_\ell = \mathbf{0}$. When other variables are held fixed, $\underline{\mathbf{Y}}$ is still optimally determined as in (28); notice that updating $\mathbf{Y}_{\ell k}$ requires computing the matrix inverse $\mathbf{U}_{\ell k} \in \mathbb{C}^{M_{\ell k} \times M_{\ell k}}$, but this is tolerable since the number of receiver antennas $M_{\ell k}$ is typically a small integer¹. With the optimal $\underline{\tilde{\mathbf{Z}}} = \underline{\tilde{\mathbf{Y}}}$ plugged in $g_s(\underline{\mathbf{W}}, \underline{\mathbf{\Gamma}}, \underline{\mathbf{Y}}, \underline{\tilde{\mathbf{Y}}}, \underline{\tilde{\mathbf{Z}}}, \underline{\mathbf{Z}})$, we can find the optimal update of $\mathbf{W}_{\ell k}$ as

$$\mathbf{W}_{\ell k}^* = \arg \min_{\underline{\mathbf{W}} \in \mathcal{W}} \|\lambda_\ell \mathbf{W}_{\ell k} - \mathbf{\Lambda}_{\ell k} - (\lambda_\ell \mathbf{I} - \mathbf{L}_\ell) \mathbf{Z}_{\ell k}\|_F^2, \\ = \mathcal{P}_{\mathcal{W}} \left(\mathbf{Z}_{\ell k} + \frac{1}{\lambda_\ell} (\mathbf{\Lambda}_{\ell k} - \mathbf{L}_\ell \mathbf{Z}_{\ell k}) \right). \quad (59)$$

Equivalently, the optimal $\underline{\mathbf{W}}$ can be obtained as

$$\mathbf{W}_{\ell k}^* = \begin{cases} \widehat{\mathbf{W}}_{\ell k} & \text{if } \sum_{j=1}^K \|\widehat{\mathbf{W}}_{\ell j}\|_F^2 \leq P_{\max} \\ \sqrt{\frac{P_\ell}{\sum_{j=1}^K \|\widehat{\mathbf{W}}_{\ell j}\|_F^2}} \widehat{\mathbf{W}}_{\ell k} & \text{otherwise,} \end{cases} \quad (60)$$

where

$$\widehat{\mathbf{W}}_{\ell k} = \mathbf{Z}_{\ell k} + \frac{1}{\lambda_\ell} (\mathbf{\Lambda}_{\ell k} - \mathbf{L}_\ell \mathbf{Z}_{\ell k}). \quad (61)$$

After $\underline{\mathbf{Z}}$ has been optimally updated to $\underline{\mathbf{W}}$, we obtain the optimal update of $\underline{\mathbf{Y}}$ as

$$\tilde{\mathbf{Y}}_{\ell k}^* = \arg \min \|\tilde{\lambda}_\ell \tilde{\mathbf{Y}}_{\ell k} - 2T \beta_\ell \dot{\mathbf{G}}_{\ell \ell} \mathbf{W}_{\ell k} - (\tilde{\lambda}_\ell \mathbf{I} - \hat{\mathbf{Q}}_\ell) \tilde{\mathbf{Z}}_{\ell k}\|_F^2 \\ = \tilde{\mathbf{Z}}_{\ell k} + \frac{1}{\tilde{\lambda}_\ell} (2T \beta_\ell \dot{\mathbf{G}}_{\ell \ell} \mathbf{W}_{\ell k} - \hat{\mathbf{Q}}_\ell \tilde{\mathbf{Z}}_{\ell k}). \quad (62)$$

Algorithm 2 summarizes the above steps and is referred to as the nonhomogeneous FP method for the ISAC beamforming. Differing from the extended WMMSE algorithm in Algorithm 1, the above new algorithm does not require computing any

¹If the number of receive antennas $M_{\ell k}$ is also a large number, then we need to apply the nonhomogeneous bound in Lemma 1 one more time so as to eliminate matrix inverse from the iterative update of $\mathbf{Y}_{\ell k}$. We omit the detail of this extension since its idea is straightforward.

Algorithm 2 Nonhomogeneous FP for ISAC Beamforming

- 1: Initialize $\underline{\mathbf{W}}$ to a feasible value, $\underline{\mathbf{Y}}$ according to (29), and $\underline{\mathbf{Z}}$ according to (57).
 - 2: **repeat**
 - 3: Update each $\mathbf{Z}_{\ell k}$ by (58).
 - 4: Update each $\Gamma_{\ell k}$ by (24).
 - 5: Update each $\mathbf{Y}_{\ell k}$ and $\tilde{\mathbf{Y}}_{\ell k}$ by (28) and (62), respectively.
 - 6: Update each $\tilde{\mathbf{Z}}_{\ell k}$ by (57).
 - 7: Update each $\mathbf{W}_{\ell k}$ by (60).
 - 8: **until** the objective value converges
-

large matrix inverse, thanks to the nonhomogeneous bound in Lemma 1.

Notice that Algorithm 2 is basically a composite application of the Lagrangian dual transform in Proposition 1, the quadratic transform in Proposition 2, and the nonhomogeneous bound in Lemma 1. In particular, it has been shown in [40] that the above transformation techniques can all be interpreted as the MM procedure, so their combination, Algorithm 2, is an MM method as well. As such, the convergence of Algorithm 2 can be immediately verified by the MM theory.

Proposition 3 (Convergence Analysis): Algorithm 2 can be interpreted as an MM method, i.e., $g_s(\underline{\mathbf{W}}, \underline{\Gamma}, \underline{\mathbf{Y}}, \tilde{\mathbf{Y}}, \underline{\mathbf{Z}}, \tilde{\mathbf{Z}})$ in (56) amounts to a surrogate function of the original objective function in (13a). Thus, according to [3], [43], Algorithm 2 is guaranteed to converge to a stationary point of problem (13), with the original objective value monotonically increasing after every iteration.

We further compare the per-iteration complexities of Algorithm 1 and Algorithm 2 in the following. To make the complexity analysis tractable, we assume that every $N_\ell^t = N_t$, every $N_\ell^r = N_r$, and every $d_{\ell k} = d$. We first focus on the update of each $\mathbf{W}_{\ell k}$. For Algorithm 1, the main complexity comes from (34) and (35), which is $\mathcal{O}(tN_t^3 + td^2N_t) = \mathcal{O}(N_t^3)$, where t is the bisection iteration that is needed to find the optimal η_ℓ . The main complexity of the proposed method comes from the eigenvalue computing, (61) and (60). We employ the power method for eigenvalue computation. Its complexity is $\mathcal{O}(cN_t^2) = \mathcal{O}(N_t^2)$, where c is the number of iterations required. The overall complexity of the two updates (60) and (61) equals $\mathcal{O}(dN_t^2 + d^2N_t)$. Therefore, the complexity of our proposed method is $\mathcal{O}(N_t^2)$. The complexity of the proposed method is much lower than the conventional method since in practice d is much smaller than N_t . Likewise, when updating $\underline{\mathbf{Y}}$, the complexity of the conventional method is $\mathcal{O}(N_r^3)$, while the complexity of the proposed method is only $\mathcal{O}(N_r^2)$.

E. Proposed Fast FP for ISAC Beamforming

In this work, we not only aim to eliminate large matrix inverse in order to reduce the per-iteration complexity (as already done in Section III-D), but also seek to accelerate the convergence in iterations. Our approach is based upon the following crucial observation: Algorithm 2 has a deep con-

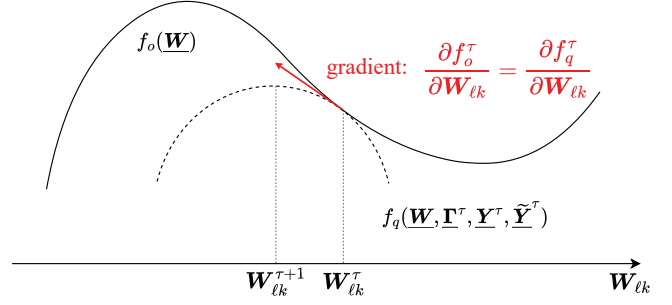


Fig. 2. In the τ th iteration, f_q and f_o have the same gradient with respect to each $\mathbf{W}_{\ell k}$ after the updates of the auxiliary variables $(\underline{\Gamma}, \underline{\mathbf{Y}}, \tilde{\mathbf{Y}})$.

nection with gradient projection, so Nesterov's extrapolation strategy comes into play.

First and foremost, we describe the connection between Algorithm 2 and gradient projection in the following proposition.

Proposition 4: Algorithm 2 is equivalent to a gradient projection, i.e., updating the primal variable $\mathbf{W}_{\ell k}$ iteratively as in (60) amounts to

$$\mathbf{W}_{\ell k}^{\tau+1} = \mathcal{P}_{\mathcal{W}} \left(\mathbf{W}_{\ell k}^{\tau} + \zeta^{\tau} \cdot \frac{\partial f_o(\mathbf{W}^{\tau})}{\partial \mathbf{W}_{\ell k}} \right), \quad (63)$$

where τ is the iteration index, $\zeta^{\tau} > 0$ is the gradient step size in the τ th iteration, and $f_o(\mathbf{W}^{\tau})$ is the primal objective function (13a).

Proof: It is difficult to compute the partial derivative $\partial f_o(\mathbf{W}^{\tau}) / \partial \mathbf{W}_{\ell k}$ directly. We suggest taking advantage of a property of the surrogate function. Recall that f_q in (25) is a surrogate function of the original objective function f_o . According to the MM theory, $f_o \geq f_q$ where the equality holds only after one round of the auxiliary variable updates have been finished. In other words, the gap between f_o and f_q is minimized to be zero at this point, so we have

$$\frac{\partial (f_o^{\tau} - f_q^{\tau})}{\partial \mathbf{W}_{\ell k}} = \mathbf{0}, \text{ for any } (\ell, k) \quad (64)$$

in the τ th iteration, where the superscript τ is the iteration index. Thus, as illustrated in Fig. 2, we further have

$$\frac{\partial f_o^{\tau}}{\partial \mathbf{W}_{\ell k}} = \frac{\partial f_q^{\tau}}{\partial \mathbf{W}_{\ell k}}. \quad (65)$$

Importantly, it turns out that the partial derivative of f_q can be easily obtained as

$$\begin{aligned} \frac{\partial f_o^{\tau}}{\partial \mathbf{W}_{\ell k}} &= \frac{\partial f_q(\mathbf{W}^{\tau}, \underline{\Gamma}^{\tau}, \underline{\mathbf{Y}}^{\tau}, \tilde{\mathbf{Y}}^{\tau})}{\partial \mathbf{W}_{\ell k}} \\ &= \Lambda_{\ell k}^{\tau} - \mathbf{L}_{\ell}^{\tau} \mathbf{W}_{\ell k}^{\tau}, \end{aligned} \quad (66)$$

where $\Lambda_{\ell k}$ and \mathbf{L}_{ℓ} are defined as in (26) and (31) with $(\underline{\Gamma}^{\tau}, \underline{\mathbf{Y}}^{\tau}, \tilde{\mathbf{Y}}^{\tau})$.

We then shift our attention to the iterative update of $\mathbf{W}_{\ell k}$ in (59) by Algorithm 2:

$$\mathbf{W}_{\ell k}^{\tau+1} = \mathcal{P}_{\mathcal{W}} \left(\mathbf{Z}_{\ell k}^{\tau} + \frac{1}{\lambda_{\ell}^{\tau}} (\Lambda_{\ell k}^{\tau} - \mathbf{L}_{\ell}^{\tau} \mathbf{Z}_{\ell k}^{\tau}) \right)$$

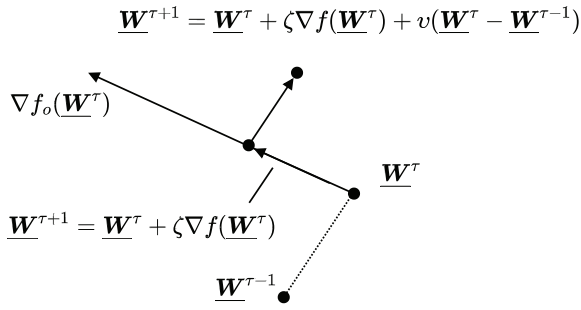


Fig. 3. Nesterov's gradient ascent with extrapolation [4].

$$\stackrel{(a)}{=} \mathcal{P}_{\mathcal{W}} \left(\mathbf{W}_{\ell k}^{\tau} + \frac{1}{\lambda_{\ell}^{\tau}} \left(\mathbf{\Lambda}_{\ell k}^{\tau} - \mathbf{L}_{\ell}^{\tau} \mathbf{W}_{\ell k}^{\tau} \right) \right)$$

$$\stackrel{(b)}{=} \mathcal{P}_{\mathcal{W}} \left(\mathbf{W}_{\ell k}^{\tau} + \frac{1}{\lambda_{\ell}^{\tau}} \cdot \frac{\partial f_o(\mathbf{W}^{\tau})}{\partial \mathbf{W}_{\ell k}^{\tau}} \right),$$

where step (a) follows by the optimal update of $\mathbf{Z}_{\ell k}$ in (57), and step (b) follows by the combination of (65) and (66). The proof is then completed. \blacksquare

Remark 3: Although the previous works [39], [40] already explored the connection between FP and gradient projection, they only consider eliminating the matrix inverse for the iterative update of $\mathbf{W}_{\ell k}$, with the nonhomogenous bound applied only once. In other words, if we stop at $g_o(\underline{\mathbf{W}}, \underline{\mathbf{\Gamma}}, \underline{\mathbf{Y}}, \underline{\mathbf{Z}})$ in (51) and consider optimizing these variables iteratively, then we would recover the results in [40]. In contrast, Algorithm 2 applies the nonhomogeneous bound twice in order to eliminate the matrix inverse for both $\mathbf{W}_{\ell k}$ and $\tilde{\mathbf{Y}}_{\ell k}$. Surprisingly, we have shown that the connection with gradient projection continues to hold after two uses of the nonhomogeneous bound. Moreover, we remark that it is difficult to carry over the relevant proofs in [39] and [40] to our problem case directly. The proof of Proposition 4 is based on a new idea.

In light of the connection between Algorithm 2 and gradient projection, we can readily accelerate Algorithm 2 by using Nesterov's extrapolation strategy [4]—which was initially designed for the gradient method. As illustrated in Fig. 3, we now extrapolate each $\mathbf{W}_{\ell k}$ along the direction of the difference between the preceding two iterates before the gradient projection, i.e.,

$$\mathbf{V}_{\ell k}^{\tau-1} = \mathbf{W}_{\ell k}^{\tau-1} + v^{\tau-1}(\mathbf{W}_{\ell k}^{\tau-1} - \mathbf{W}_{\ell k}^{\tau-2}), \quad (67)$$

$$\mathbf{W}_{\ell k}^{\tau} = \mathcal{P}_{\mathcal{W}} \left(\mathbf{V}_{\ell k}^{\tau-1} + \frac{1}{\lambda_{\ell}^{\tau}} (\mathbf{\Lambda}_{\ell k} - \mathbf{L}_{\ell} \mathbf{V}_{\ell k}^{\tau-1}) \right), \quad (68)$$

where τ is the iteration index, the extrapolation step v_{τ} is chosen as

$$v^{\tau} = \max \left\{ \frac{\tau - 2}{\tau + 1}, 0 \right\}, \quad \text{for } \tau = 1, 2, \dots, \quad (69)$$

the starting point is $\underline{\mathbf{W}}^{-1} = \underline{\mathbf{W}}^0$. Algorithm 3 summarizes the above steps and is referred to as the fast FP algorithm.

IV. NUMERICAL RESULTS

We validate the performance of the proposed algorithms numerically in a 7-cell wrapped-hexagonal-around network.

Algorithm 3 Fast FP for ISAC Beamforming

- 1: Initialize $\underline{\mathbf{W}}$ to a feasible value, $\underline{\tilde{\mathbf{Y}}}$ according to (29), and $\underline{\tilde{\mathbf{Z}}}$ according to (57).
 - 2: **repeat**
 - 3: Update each $\mathbf{V}_{\ell k}$ according to (67) and set $\mathbf{W}_{\ell k} = \mathbf{V}_{\ell k}$.
 - 4: Update each $\mathbf{Z}_{\ell k}$ by (58).
 - 5: Update each $\mathbf{\Gamma}_{\ell k}$ by (24).
 - 6: Update each $\mathbf{Y}_{\ell k}$ and $\tilde{\mathbf{Y}}_{\ell k}$ by (28) and (62), respectively.
 - 7: Update each $\tilde{\mathbf{Z}}_{\ell k}$ by (57).
 - 8: Update each $\mathbf{W}_{\ell k}$ by (60).
 - 9: **until** the objective value converges
-

Within each cell, the BS is located at the center, with the BS-to-BS distance being 800 meters, while its associated downlink users are randomly distributed; we make the downlink users be close to the cell edge on purpose in order to stress the cross-cell interference effect. Let every BS have the same number of transmit (resp. receive) antennas denoted by N_t (resp. N_r). Let every downlink user have 4 antennas; 4 data streams are intended for each of them. The maximum transmit power P_{ℓ} at each BS is set to 20 dBm, the background noise power level at the downlink user side σ^2 is -80 dBm, and the background noise power level at the BS side $\tilde{\sigma}^2$ is set to 0 dBm. The downlink distance-dependent path-loss is given by $15.3 + 37.6 \log_{10}(d) + \xi$ (in dB), where d represents the BS-to-user distance in meters, and ξ is a zero-mean Gaussian random variable with a standard variance of 8 dB—which models the shadowing effect. For the sensing, every reflection coefficient $\xi_{\ell i}$ is set to 1 as in [44]–[46]. The block length T equals 30. We use the same starting point for all the competitor algorithms for the comparison fairness.

A. Convergence Rate

We begin with the convergence speed performance of the various methods in solving problem (13). Assume that there are 45 downlink users in each cell. The priority weights in problem (13) are set as $\beta_{\ell} = 10^{-11}$ and $\omega_{\ell k} = 1$. (Notice that β_{ℓ} is considerably smaller because the Fisher information value is usually much greater than the data rate value.)

Fig. 4 shows the convergence behaviors of the different algorithms when $N_t = N_r = 128$, i.e., when both transmit antennas and radar antennas are massively deployed. Observe from Fig. 4(a) that the extended WMMSE converges faster than the nonhomogeneous FP and the fast FP in iterations. From an MM perspective, this is because the extended WMMSE gives a tighter approximation of the original objective function $f_o(\underline{\mathbf{W}})$. However, this does not imply that the absolute running time of the extended WMMSE is the shortest, because in the meanwhile the extended WMMSE requires heavier computations per iteration due to the large matrix inversion. Actually, it can be seen from Fig. 4(b) that the nonhomogeneous FP converges faster than extended WMMSE in time. For example, extended WMMSE requires about 23 seconds to reach the objective value of 158, while

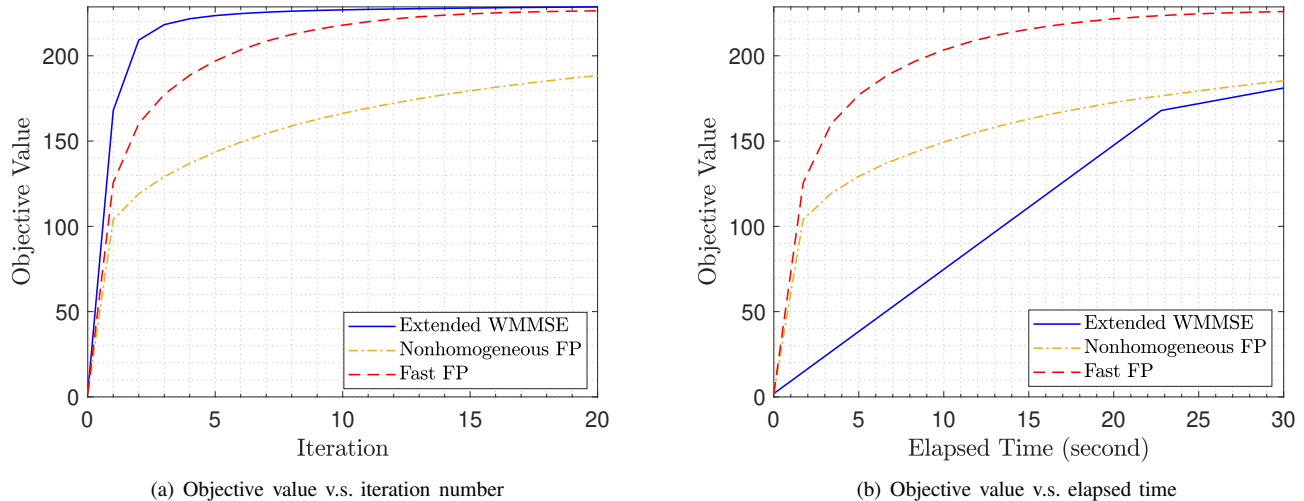


Fig. 4. The convergence behaviors of the different ISAC beamforming algorithms when $N_r = N_t = 128$.

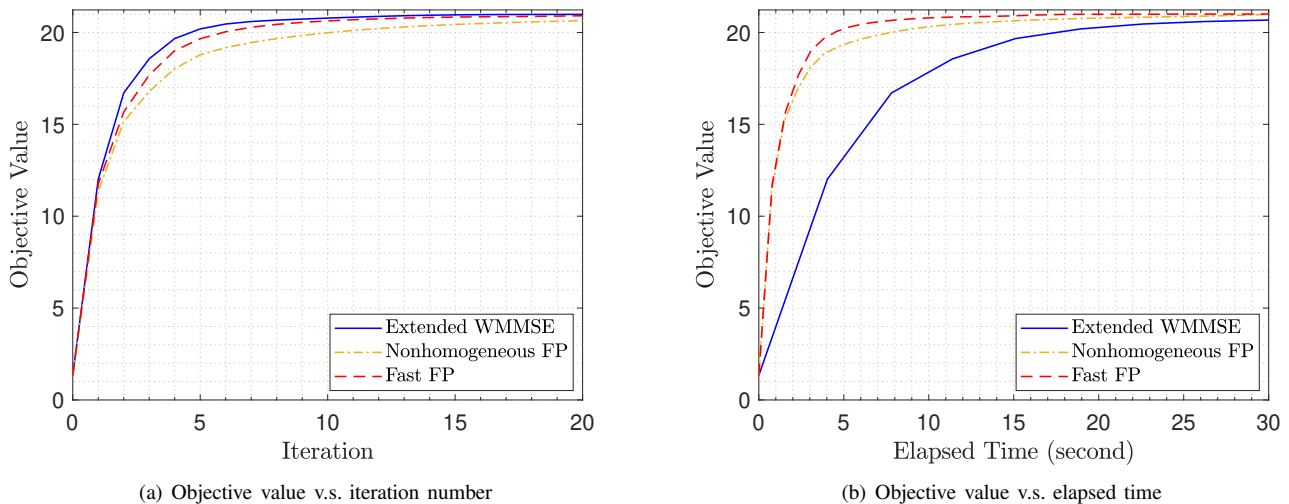


Fig. 5. The convergence behaviors of the different ISAC beamforming algorithms when $N_r = N_t = 4$.

the nonhomogeneous FP merely requires 18 seconds. Thus, in practice, the nonhomogeneous FP still runs much faster than the extended WMMSE. Further, observe also that the fast FP outperforms the nonhomogeneous FP not only in terms of the iteration efficiency but also in terms of the time efficiency. For example, to reach the objective value of 160, the nonhomogeneous FP requires 8 iterations and 14 seconds, while the fast FP just requires 2 iterations and 3.5 seconds. Thus, the fast FP can further improve upon the nonhomogeneous FP significantly, thanks to Nesterov's acceleration strategy. Moreover, we consider in Fig. 5 the small-antenna-array case of $N_t = N_r = 4$. According to the figure, although the advantage of the fast FP over the nonhomogeneous FP now becomes smaller, it still outperforms the extended WMMSE significantly in terms of running time.

B. Angle Estimation Performance

Next, we focus on the sensing performance by considering the estimation of θ_ℓ under the different ISAC beamforming algorithms. The transmit power of each BS is fixed at 10 dBm. Let $N_t = N_r = 128$; let each $\beta_\ell = 10^{-8}$ and let each $\omega_{\ell k} = 1$; we now adopt a larger weight β_ℓ for sensing than in Section IV-A so as to highlight the sensing performance. Now assume that each cell contains a total of 15 downlink users. Consider the following 5 possible target positions as depicted in Fig. 6:

- Position a: (500m, -1000m)
- Position b: (300m, -900m)
- Position c: (800m, 900m)
- Position d: (500m, 500m)
- Position e: (100m, -300m)

We shall sequentially place the target at the above positions.

The angle estimation method comes from [47], as briefly described in the following for completeness. Let \mathbf{X}_ℓ be the

TABLE II
ESTIMATING θ_ℓ FOR THE POINT TARGET AT 5 DIFFERENT POSITIONS

Target Position	Mean Squared Error					Max Squared Error				
	a	b	c	d	e	a	b	c	d	e
Extended WMMSE	0.0458	0.1763	0.0379	0.0125	0.0643	0.1633	0.9471	0.1068	0.0452	0.3199
Nonhomogeneous FP	0.0228	0.0059	0.0097	0.0091	0.0112	0.0795	0.0114	0.0248	0.0248	0.0238
Proposed Fast FP	0.0123	0.0059	0.0097	0.0091	0.0112	0.0309	0.0114	0.0248	0.0248	0.0238

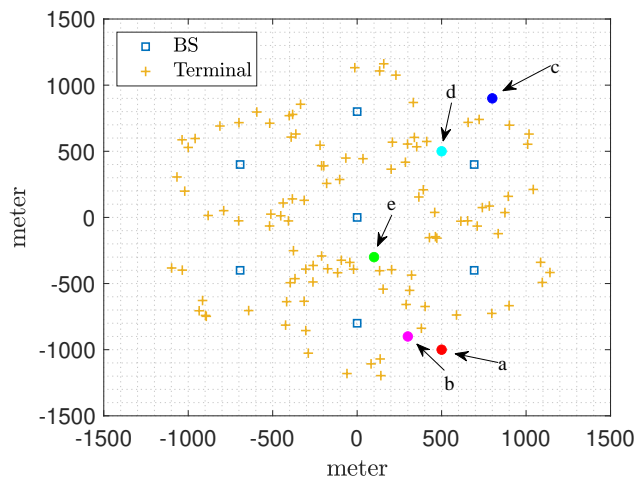


Fig. 6. Positions of BSs, downlink users, and the sensing targets in a 7-cell wrapped-around ISAC network.

transmit signal of BS ℓ , i.e., $\mathbf{X}_\ell = \sum_k \mathbf{W}_{\ell k} \mathbf{S}_{\ell k}$. The θ_ℓ estimate is given by

$$\hat{\theta}_\ell = \arg \max_{\theta_\ell} \frac{|\text{tr}(\mathbf{G}_{\ell, \ell}(\theta_\ell)^H \tilde{\Psi}_\ell \mathbf{X}_\ell^H)|^2}{\text{tr}((\mathbf{G}_{\ell \ell}(\theta_\ell) \mathbf{X}_\ell)^H (\mathbf{G}_{\ell \ell}(\theta_\ell) \mathbf{X}_\ell))}. \quad (70)$$

In particular, to account for time efficiency, we carry out each algorithm under a time-limited setting, i.e., the running time is limited to 2.5 seconds. Regarding the estimation error metric, we consider two choices: (i) the mean squared error $\frac{1}{L} \sum_\ell |\hat{\theta}_\ell - \theta_\ell|^2$ and (ii) the max squared error $\max_\ell |\hat{\theta}_\ell - \theta_\ell|^2$. The performance of the different algorithms is summarized in Table II. Observe from Table II that the extended WMMSE has the worst performance. For example, at position a, the nonhomogeneous FP reduces the mean squared error by about 50% as compared to the extended WMMSE, while the fast FP reduces by about 73%. Thus, although all the algorithms can guarantee convergence to the stationary point, the extended WMMSE is much more time consuming and thus is inferior to the other two methods when the running time is limited. It is worth noticing that the nonhomogeneous FP and the fast FP end up with the same estimation error for most target positions, but the latter achieves a higher objective value than the former. The reason is that the mean squared error and the max squared error are sensitive to the specific estimation algorithm; clearly, the estimation algorithm [47] we adopt does not differ much between the nonhomogeneous FP and the fast FP. In contrast, according to the general metric of the Fisher information that

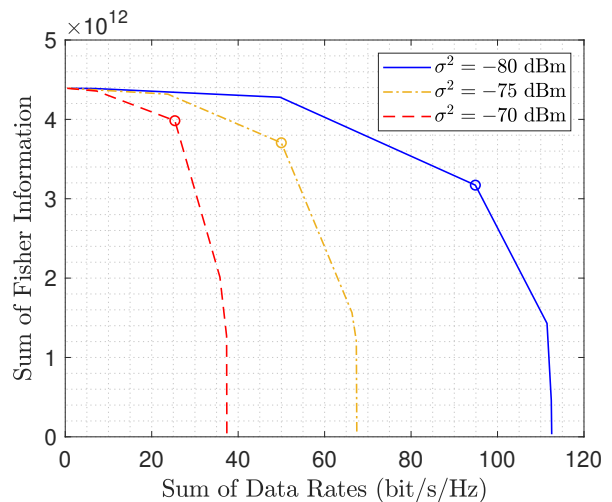


Fig. 7. Tradeoff between the sum of rates and the sum of Fisher information by varying the value of $\omega_{\ell k}$ while fixing $\beta_\ell = 10^{-11}$. The circled points stand for the case with each $\omega_{\ell k} = 0.1$.

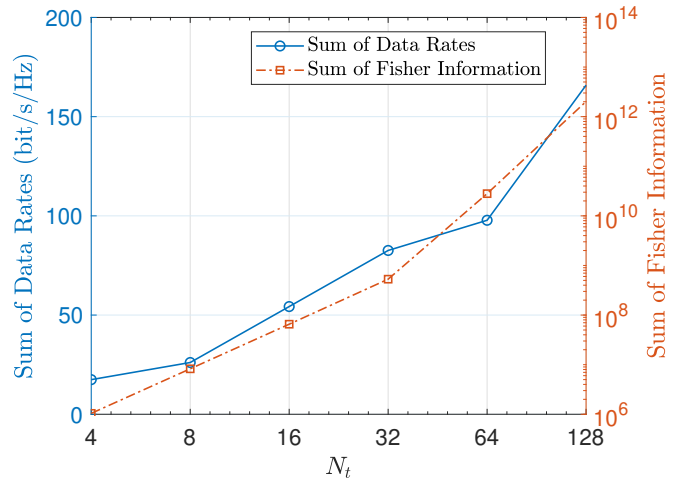


Fig. 8. The sum of data rates vs. the sum of Fisher information vs. N_t .

is independent of the specific estimation algorithm, the fast FP still outperforms the nonhomogeneous FP, as shown in the previous simulation results.

C. Communications v.s. Sensing

Lastly, we examine the tradeoff between the communications performance and the sensing performance. We now assume that there are 6 downlink users in each cell. Fig. 7

shows the tradeoff curve between the sum of data rates and the sum of Fisher information under the different noisy environments. To enable tradeoff, we fix the sensing weights β_ℓ at 10^{-11} while varying the communications weights $\omega_{\ell k}$ ranging from 10^{-10} to 10^{10} . Notice that the tradeoff curves meet at the same point when $\omega_{\ell k}$ tends to 10^{-10} so that the beamforming is considered for sensing alone. When we start to put more weights on communications, the three curves start to diverge. The figure shows that the sum of data rates increases most rapidly with $\omega_{\ell k}$ raised to 0.1 when $\sigma^2 = -80$ dBm, i.e., in the high-SNR regime. Moreover, regardless of the noise power level σ^2 , as the communications weights get higher, we always observe that the growth of data rates is fast at the beginning and then slows down.

Furthermore, we look into the ISAC objective more closely by plotting the sum of data rates and the sum of Fisher information separately in Fig. 8 for the different choices of the number of transmit antennas N_t . We now assume that there are 30 downlink users in each cell. Notice that the sum of data rates enhances with N_t linearly at most of the time. For example, when N_t increases from 8 to 16, the sum of data rates is doubled approximately. In comparison, the improvement of the Fisher information is much sharper. For example, when N_t increases from 8 to 16, the sum of the Fisher information is enhanced by almost an order of magnitude. Thus, our method is capable of reaping the DoF gain when the large antenna arrays are deployed.

V. CONCLUSION

This paper considers the ISAC beamforming optimization for a multi-cell massive MIMO network. Based on the FP technique, we first extend the classic WMMSE algorithm from the communications case to the ISAC case. This approach works but at a high cost of computation because the extended WMMSE requires inverting large matrices. We then develop the non-homogeneous bound to eliminate the large matrix inversion from the extended WMMSE (which can be also viewed as an FP based method). As a result, the per-iteration complexity can be significantly reduced. Furthermore, we show that the above FP based method is connected to gradient projection, and then propose using Nesterov's extrapolation scheme to render the beamforming algorithm converge much more rapidly.

REFERENCES

- [1] S. S. Christensen, R. Agarwal, E. D. Carvalho, and J. M. Cioffi, "Weighted sum-rate maximization using weighted MMSE for MIMO-BC beamforming design," *IEEE Trans. Wireless Commun.*, vol. 7, no. 12, pp. 4792–4799, Dec. 2008.
- [2] Q. Shi, M. Razaviyayn, Z.-Q. Luo, and C. He, "An iteratively weighted mmse approach to distributed sum-utility maximization for a MIMO interfering broadcast channel," *IEEE Trans. Signal Process.*, vol. 59, no. 9, pp. 4331–4340, Sept. 2011.
- [3] Y. Sun, P. Babu, and D. P. Palomar, "Majorization-minimization algorithms in signal processing, communications, and machine learning," *IEEE Trans. Signal Process.*, vol. 65, no. 3, pp. 794–816, Aug. 2016.
- [4] Y. Nesterov, *Lectures on Convex Optimization (Second Edition)*. Springer, 2018.
- [5] R. Saruthirathanaworakun, J. M. Peha, and L. M. Correia, "Opportunistic sharing between rotating radar and cellular," *IEEE J. Sel. Areas Commun.*, vol. 30, no. 10, pp. 1900–1910, Nov. 2012.
- [6] D. Ma, N. Shlezinger, T. Huang, Y. Liu, and Y. C. Eldar, "Joint radar-communication strategies for autonomous vehicles: Combining two key automotive technologies," *IEEE Signal Process. Mag.*, vol. 37, no. 4, pp. 85–97, July 2020.
- [7] T. Huang, N. Shlezinger, X. Xu, Y. Liu, and Y. C. Eldar, "MAJoRCom: A dual-function radar communication system using index modulation," *IEEE Trans. Signal Process.*, vol. 68, pp. 3423–3438, May 2020.
- [8] X. Liu, T. Huang, N. Shlezinger, Y. Liu, J. Zhou, and Y. C. Eldar, "Joint transmit beamforming for multiuser MIMO communications and MIMO radar," *IEEE Trans. Signal Process.*, vol. 68, pp. 3929–3944, June 2020.
- [9] Z. He, W. Xu, H. Shen, D. W. K. Ng, Y. C. Eldar, and X. You, "Full-duplex communication for ISAC: Joint beamforming and power optimization," *IEEE J. Sel. Areas Commun.*, vol. 11, no. 9, pp. 2920–2936, June 2023.
- [10] F. Liu, Y. Liu, A. Li, C. Masouros, and Y. C. Eldar, "Cramér-Rao bound optimization for joint radar-communication beamforming," *IEEE Trans. Signal Process.*, vol. 70, pp. 240–253, Dec. 2021.
- [11] X. Wang, Z. Fei, J. A. Zhang, and J. Xu, "Partially-connected hybrid beamforming design for integrated sensing and communication systems," *IEEE Trans. Commun.*, vol. 70, no. 10, pp. 6648–6660, Oct. 2022.
- [12] Z. Wang, J. Wu, Y.-F. Liu, and F. Liu, "Globally optimal beamforming design for integrated sensing and communication systems," in *Proc. IEEE Int. Conf. Acoust., Speech, Signal Process. (ICASSP)*, Apr. 2024, pp. 8931–8935.
- [13] B. Guo, J. Liang, G. Wang, B. Tang, and H. So, "Bistatic MIMO DFRC system waveform design via fractional programming," *IEEE Trans. Signal Process.*, vol. 71, pp. 1952–1967, May 2023.
- [14] M. Zhu, L. Li, S. Xia, and T.-H. Chang, "Information and sensing beamforming optimization for multi-user multi-target MIMO ISAC systems," *EURASIP Journal Adv. Signal Process.*, vol. 2023, no. 1, p. 15, Jan 2023.
- [15] B. Guo, J. Liang, B. Tang, L. Li, and H. C. So, "Bistatic MIMO DFRC system waveform design via symbol distance/direction discrimination," *IEEE Trans. Signal Process.*, vol. 71, pp. 3996–4010, Oct. 2023.
- [16] S. Liu, M. Li, R. Liu, W. Wang, and Q. Liu, "Joint transmit beamforming and receive filter design for cooperative multi-static ISAC networks," *IEEE Wireless Commun. Lett.*, Apr. 2024.
- [17] R. Li, Z. Xiao, and Y. Zeng, "Towards seamless sensing coverage for cellular multi-static integrated sensing and communication," *IEEE Trans. Wireless Commun.*, Oct. 2023.
- [18] N. Su, F. Liu, and C. Masouros, "Sensing-assisted eavesdropper estimation: An ISAC breakthrough in physical layer security," *IEEE Trans. Wireless Commun.*, Aug. 2023.
- [19] Z. Wang, X. Mu, and Y. Liu, "STARS enabled integrated sensing and communications," *IEEE Trans. Wireless Commun.*, vol. 22, no. 10, pp. 6750–6765, Oct. 2023.
- [20] Z. Behdad, Ö. T. Demir, K. W. Sung, E. Björnson, and C. Cavdar, "Power allocation for joint communication and sensing in cell-free massive MIMO," in *Proc. IEEE Global Commun. Conf. (GLOBECOM)*, Dec. 2022, pp. 4081–4086.
- [21] R. Liu, M. Li, Q. Liu, and A. L. Swindlehurst, "SNR/CRB-constrained joint beamforming and reflection designs for RIS-ISAC systems," *IEEE Trans. Wireless Commun.*, 2023.
- [22] Z. Yu, H. Ren, C. Pan, G. Zhou, B. Wang, M. Dong, and J. Wang, "Active RIS aided ISAC systems: Beamforming design and performance analysis," *IEEE Trans. Commun.*, Nov. 2023.
- [23] G. Cheng, Y. Fang, J. Xu, and D. W. K. Ng, "Optimal coordinated transmit beamforming for networked integrated sensing and communications," *IEEE Trans. Wireless Commun.*, Jan. 2024.
- [24] Z. Zhou, X. Li, G. Zhu, J. Xu, K. Huang, and S. Cui, "Integrating sensing, communication, and power transfer: Multiuser beamforming design," *IEEE J. Sel. Areas Commun.*, to be published.
- [25] X. Li, F. Liu, Z. Zhou, G. Zhu, S. Wang, K. Huang, and Y. Gong, "Integrated sensing, communication, and computation over-the-air: MIMO beamforming design," *IEEE Trans. Wireless Commun.*, vol. 22, no. 8, pp. 5383–5398, 2023.
- [26] N. Huang, H. Dong, C. Dou, Y. Wu, L. Qian, S. Ma, and R. Lu, "Edge intelligence oriented integrated sensing and communication: A multi-cell cooperative approach," *IEEE Trans. Veh. Technol.*, Jan. 2024.
- [27] K. Meng, Q. Wu, S. Ma, W. Chen, K. Wang, and J. Li, "Throughput maximization for UAV-enabled integrated periodic sensing and communication," *IEEE Trans. Wireless Commun.*, vol. 22, no. 1, pp. 671–687, Aug. 2022.
- [28] M. Hua, Q. Wu, W. Chen, O. A. Dobre, and A. L. Swindlehurst, "Secure intelligent reflecting surface aided integrated sensing and communication,"

- tion," *IEEE Trans. Wireless Commun.*, vol. 23, no. 1, pp. 575–591, Jan 2024.
- [29] Y. Guo, Y. Liu, Q. Wu, X. Li, and Q. Shi, "Joint beamforming and power allocation for RIS aided full-duplex integrated sensing and uplink communication system," *IEEE Trans. Wireless Commun.*, Oct. 2023.
- [30] Z. Chen, J. Wang, Z. Tian, M. Wang, Y. Jia, and T. Q. Quek, "Joint rate splitting and beamforming design for RSMA-RIS-assisted ISAC system," *IEEE Wireless Commun. Lett.*, vol. 13, no. 1, pp. 173–177, Jan. 2023.
- [31] K. Shen and W. Yu, "Fractional programming for communication systems—Part II: Uplink scheduling via matching," *IEEE Trans. Signal Process.*, vol. 66, no. 10, pp. 2631–2644, Mar. 2018.
- [32] K. Shen, W. Yu, L. Zhao, and D. P. Palomar, "Optimization of MIMO device-to-device networks via matrix fractional programming: A minorization-maximization approach," *IEEE/ACM Trans. Netw.*, vol. 27, no. 5, pp. 2164–2177, Oct. 2019.
- [33] J. Zou, S. Sun, C. Masouros, Y. Cui, Y.-F. Liu, and D. W. K. Ng, "Energy-efficient beamforming design for integrated sensing and communications systems," *IEEE Trans. Commun.*, Feb. 2024.
- [34] C. Deng, X. Fang, and X. Wang, "Beamforming design and trajectory optimization for UAV-empowered adaptable integrated sensing and communication," *IEEE Trans. Wireless Commun.*, vol. 22, no. 11, pp. 8512–8526, Nov. 2023.
- [35] C. Liu, W. Yuan, S. Li, X. Liu, H. Li, D. W. K. Ng, and Y. Li, "Learning-based predictive beamforming for integrated sensing and communication in vehicular networks," *IEEE J. Sel. Areas Commun.*, vol. 40, no. 8, pp. 2317–2334, Aug. 2022.
- [36] Q. Qi, X. Chen, C. Zhong, C. Yuen, and Z. Zhang, "Deep learning-based design of uplink integrated sensing and communication," *IEEE Trans. Wireless Commun.*, Mar. 2024.
- [37] S. Fortunati, L. Sanguinetti, F. Gini, M. S. Greco, and B. Himed, "Massive MIMO radar for target detection," *IEEE Trans. Signal Process.*, vol. 68, pp. 859–871, Jan. 2020.
- [38] X. Zhao, S. Lu, Q. Shi, and Z.-Q. Luo, "Rethinking WMMSE: Can its complexity scale linearly with the number of bs antennas?" *IEEE Trans. Signal Process.*, vol. 71, pp. 433–446, Feb. 2023.
- [39] Z. Zhang, Z. Zhao, and K. Shen, "Enhancing the efficiency of WMMSE and fp for beamforming by minorization-maximization," in *Proc. IEEE Int. Conf. Acoust., Speech, Signal Process. (ICASSP)*, June 2023, pp. 1–5.
- [40] K. Shen, Z. Zhao, Y. Chen, Z. Zhang, and H. V. Cheng, "Accelerating quadratic transform and WMMSE," *IEEE J. Sel. Areas Commun.*, to be published.
- [41] D. P. Bertsekas, *Convex Optimization Algorithms*. Athena Scientific, 2015.
- [42] H. L. Van Trees, *Optimum Array Processing: Part IV of Detection, Estimation, and Modulation Theory*. Hoboken, NJ, USA: Wiley, 2002.
- [43] M. Razaviyayn, M. Hong, and Z.-Q. Luo, "A unified convergence analysis of block successive minimization methods for nonsmooth optimization," *SIAM J. Optim.*, vol. 23, no. 2, pp. 1126–1153, 2013.
- [44] Z. Cheng, B. Liao, S. Shi, Z. He, and J. Li, "Co-design for overlaid MIMO radar and downlink MISO communication systems via Cramér-Rao bound minimization," *IEEE Trans. Signal Process.*, vol. 67, no. 24, pp. 6227–6240, Dec. 2019.
- [45] Z. Ren, Y. Peng, X. Song, Y. Fang, L. Qiu, L. Liu, D. W. K. Ng, and J. Xu, "Fundamental CRB-rate tradeoff in multi-antenna ISAC systems with information multicasting and multi-target sensing," *IEEE Trans. Wireless Commun.*, Sept. 2023.
- [46] H. Hua, T. X. Han, and J. Xu, "MIMO integrated sensing and communication: CRB-rate tradeoff," *IEEE Trans. Wireless Commun.*, Aug. 2023.
- [47] X. Song, J. Xu, F. Liu, T. X. Han, and Y. C. Eldar, "Intelligent reflecting surface enabled sensing: Cramér-rao bound optimization," *IEEE Trans. Signal Process.*, May 2023.